Experimental investigation of fire spread across a vegetative fuel bed incorporating the effect of wind velocity

Reza M. Ziazi[(a)], Abhinandan Singh[(a)], Ahmed O. Said[(a)], Weixuan Gong[(a)], Bruno E. Schardong[(a)], Matthew Patterson[(b)], Nicholas S.Skowronski[(b)], Albert Simeoni[(a)]

[(a)]Department of Fire Protection Engineering, Worcester Polytechnic Institute, MA, USA 01605
[(b)]USDA Forest Service, Northern Research Station, Morgantown, WV 26505, USA

Abstract

Wind, moisture content, and density of fuel are three environmental factors that affect the rate of fire spread in wildland fires by changing the rate of convection, radiation, and conduction heat transfer from the flames and burned fuels to the unburned fuel. These effects have been experimentally investigated in the current study to further understand the complex phenomena of wildland fire spread. In this study, wind tunnel experiments have been carried out using three different wind velocities across a fuel bed comprised of pine needles heterogeneously distributed to cover an area of 1.2x3 m^2. The surface temperature of the vegetative fuel (or pine needle) has been measured using thermocouples to study the temperature variations over the fuel bed to probe the effect of upstream wind over the fuel bed. Moreover, the fuel consumption has been evaluated for a select area of 0.5x0.6m^2 using a load cell to investigate the mass loss rate of the fuel during pyrolysis, flaming, and smoldering combustion. The rate of flame spread is estimated by analyzing the temperature of the fuel bed, which was synchronized with the images captured from the flame front. The mass loss rate is seen to increase with the wind velocity. The spread rate shows a constant increase with the increased velocity, which has also influenced the variation of heat flux and temperature over the bed.

Keywords: Wildland fires, Porous media, Fuel bed, Fire spread, Pine needles, Smoldering

1. Introduction

Fires are an increasing threat on humans and ecosystems as demonstrated by the devastating wildfires that occurred over the last few years. Determination of the parameters controlling the spread of wildland fires is a key step to improve the techniques employed to manage, mitigate, and prevent such fires. The parameters include, but not limited to, type of vegetative fuel, fuel moisture content, wind speed and direction, terrain slope, etc. A series of studies have been conducted to study the impact of vegetation properties and slope on the rate of fire spread, flame geometry, temperature profile, rate of fuel consumption, and combustion products [1-7].

Understanding the linkages between fuel characteristics, fire dynamics, and air quality is necessary to develop and validate risk-reducing fire models. The objective of this study is to determine through laboratory scale combustion experiments in a wind tunnel the effect of wind velocity on fire dynamics, fuel mass loss rate, change in fuel temperature, and incident heat flux.

2. Experimental setup

Laboratory-scale fire spread experiments were conducted in a well-characterized variable-flow wind tunnel designed for fire research [8-10]. Various parameters affecting the burning behavior, namely, temperature, heat flux, and flame geometry were measured during the flame spread using appropriate instrumentation. Since the objective of this research was to develop a better understanding of the prescribed burns conducted

in the south-eastern states of the United States, the same type of longleaf pine needles (*Pinus palustris* [10]) with the density of 592.7 kg/m^3 were procured. The reconstruction of the packing structure of pine needles was controlled to be close to porosity variations in the artificially constructed fuel beds (>90%) which is slightly different from forest floor porosities [12-13]. The depth variation of the fuel bed was 5-7 cm throughout the bed. The complete experimental setup is presented in Fig. 1, while the test matrix is given in Table 1.

Table 1. Experimental test matrix along with the fuel properties

Test number	Mass of the fuel (g)	Wind velocity (m/s)	Area density (g/m^2)	Porosity	Packing ratio
Test 1	2933	1	815	97-98%	0.03
Test 2	2933	2	815	97-98%	0.03
Test 3	2933	3	815	97-98%	0.03

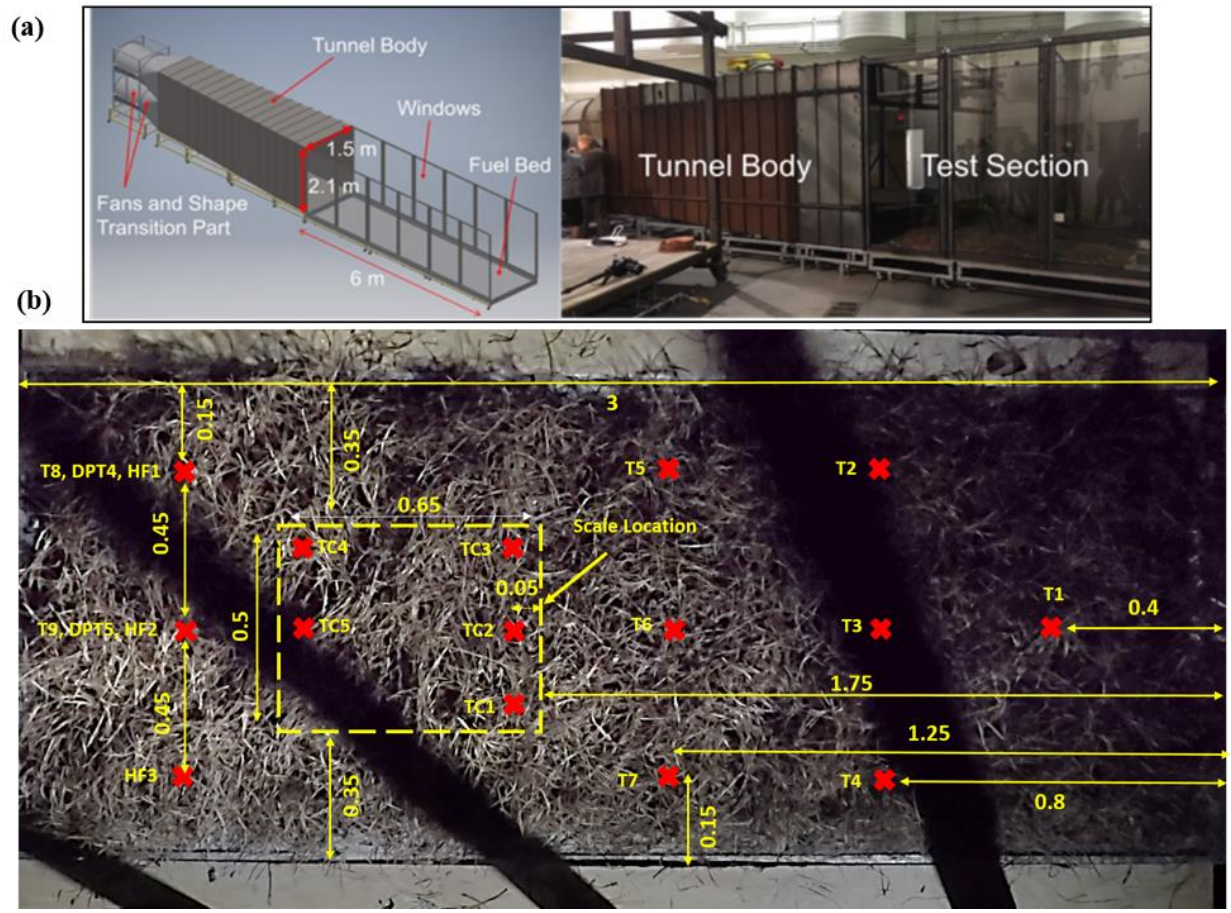

Figure 1. (a) A schematic and photograph of the variable flow wind tunnel used to establish wind-driven flames over dead pine needles uniformly spread across the fuel bed. (b) A schematic of the fuel bed with various measurement instruments used to acquire the fire spread behavior (all dimensions are in meters).

A testbed measuring 1.2m x 3m was placed inside the wind tunnel with various sensors positioned strategically to acquire the essential burning characteristics of wind-driven flames. Before each fire spread experiment, the fuel bed was covered with a thick layer of sand which served two purposes. First, it helped emulate the ground fire more accurately, and second, it prevented any excess heat transfer towards the fuel bed. The moisture content of the pine needles was measured before each test case and has been presented in Table 1. From right to left (downstream direction), thin-skin calorimeters T1 to T7 [14] were placed flush over a super wool insulation board (measuring 10 cm x 10 cm) on the testbed to measure the total heat flux values. A total of five K-type thermocouples (TC1 to TC5) were placed over the rectangular section of dimensions 0.5m x 0.65m. This rectangular section was positioned above the high-precision load cell (Adam CKT 32UH) to measure the mass-loss rate.

Figure 2. The procedure used to extract the binary images from true color images recorded at 30 frames per second.

Furthermore, three micro-thermocouples (100μm in diameter) of K-type were placed along with a Medtherm total heat flux gauge and differential pressure transducer (DPT4, DPT5) to measure the total heat flux and velocity, respectively. The analog input from various devices was acquired and digitized using LabVIEW at a sampling rate of 1Hz, with NI 9205 used for voltage measurements and NI 9213 for temperature readings.

Various video cameras (GoPro Black 5 and Black 7) with a frame rate of 30 fps were placed at side- and top-views to acquire the flame geometry throughout the burn. A robust image analysis technique was developed to analyze the spread rate of the flame by observing the flame position at different time steps. These true-color images were then individually converted into grayscale images, which were further utilized to generate a binary image profile using Otsu's method [15], as shown in Fig. 2. The flame structure for each time instant was established by averaging 30 binary frames for each time step to generate a flame probability contour profile. A probability value of P=0.5 was considered the location of the flame, following the work of Heskestad [16]. An example of probability contour profile is presented in Fig. 3.

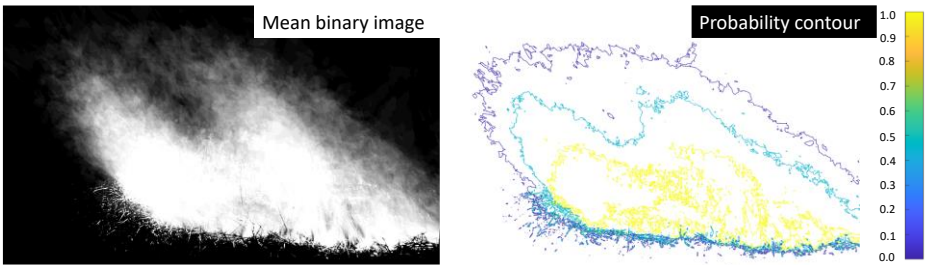

Figure 3. Conversion of the mean binary image into a probability contour profile, where P=0.5 was taken as the flame location at different time instants.

A controlled burn environment was established by placing a row of pitot tubes ahead of the testbed to measure the exact flow velocity throughout the experiment. A small sample of about 20 to 30g was taken from the prepared fuel, weighed, and oven-dried for 24h at a temperature of 105°C [17]. The oven-dried fuel sample was weighed again to evaluate the average fuel moisture content before ignition. For all the tests conducted in this study, the moisture content was kept in the range of 10-11%, similar to the values observed in the field for dry conditions. Since the ignition technique can also affect the burning behavior of wind-driven flames [18], the same ignition source was utilized for each test. A total of 30 cotton balls wrapped around a metal rod of length 400mm and soaked with liquid ethanol was placed at the leading edge of the fuel bed. A high voltage was passed through a thin nichrome wire (1mm diameter) positioned in the middle of the metal rod to ignite the cotton, which further acted as an ignition source for the dead pine needles. The electric power source was switched off immediately after the ignition of the cotton balls.

3. Results and Discussion

The main purpose of this research is focused on the flame spread characteristics in three wind velocities discussed in Section 1. The flame spread rate, temperature of the fuel over the load cell, mass loss as well as mass loss rate, and heat flux variations for three wind velocities of 1, 2, and 3 m/s are discussed.

3.1 Flame spread rate

The flame spread rate is evaluated based on the processing of the frames from the side-view camera positioned across the load-cell. The leading edge of the flame touching the fuel bed was used as a subjective method of estimating the spread rate. Since flame structure plays a crucial role in dictating the fire spread behavior in flaming self-sustaining combustion, a strong emphasis was given to accurately acquire the flame geometry. The spread rate was calculated over the load cell where the analysis of the rate is performed at the beginning of the load cell at 1.75m downstream from the ignition point. As shown in Fig. 4, the spread rate constantly increases with the wind velocity from 1 m/s to 3 m/s.

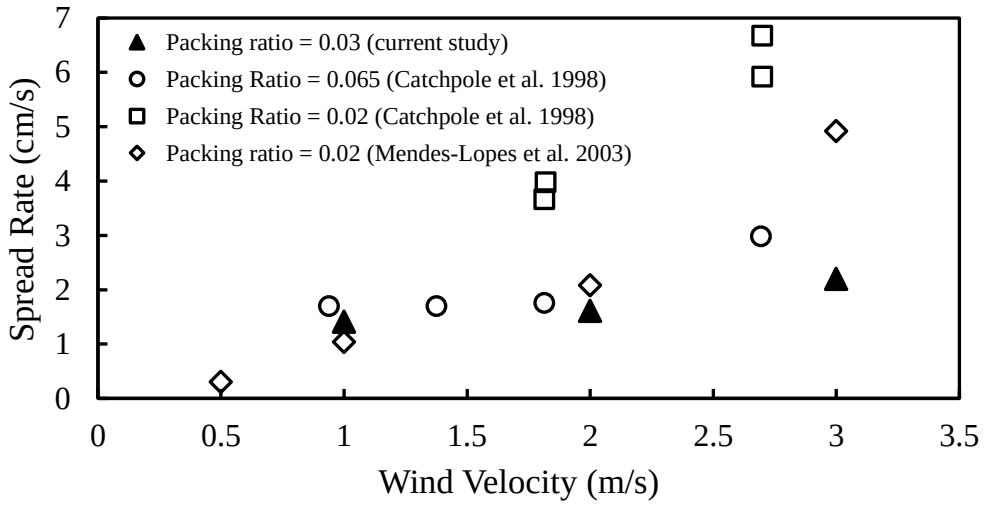

Figure 4. Spread rate at different wind tunnel velocities for the current study and the comparison with the study performed by Catchpole et al. (1998) *and Mendes-Lopez et al (2003)*.

The linear fit to the current result of the spread rate shows a slope of 0.4 with variation between 1.5 cm/s to 2.2 cm/s. A similar variation is observed by Catchpole et al. [19] for a fuel bed comprised of pine needles at a packing ratio of 0.065 with similar trend in spread rate, which varies in the range of 1.7 cm/s to 3 cm/s

for the wind velocities ranging between 1-3 m/s. However, an experiment with a slightly reduced packing ratio (0.02) performed by Catchpole et al. representants a larger spread rate with variations between 4 to 7 cm/s for the similar wind velocities. Another study performed by Mendes-Lopes et al. [5], which has used the same packing ratio (0.02), reported similar trends for the spread rate at 1, and 2 m/s, however a deviation occurred at 3m/s.

The trend of flame spread rate with wind velocity represents the constant convective effects of heat transfer on the flame over the porous bed with a certain packing ratio. Slight changes in the packing ratio changes the variation of spread rate, which could be result of the changes of the velocity gradients at boundary layer near the surface of the porous bed or due to coupled conduction-convection effects for different porosities.

3.2 Weight loss over the load cell

The weight loss trace represents the fuel consumption by the flame in different wind velocities which promotes to understand the fuel bed characteristics in the three phases of pylrolysis, flaming, and smoldering. The instantaneous mass loss at a frequency of 2 Hz was investigated for the three wind velocities throughout the time from the start of ignition as shown in Fig. 5. The total weight loss for the three velocities of 1,2, and 3m/s are 197, 191.2, and 210.8g, respectively.

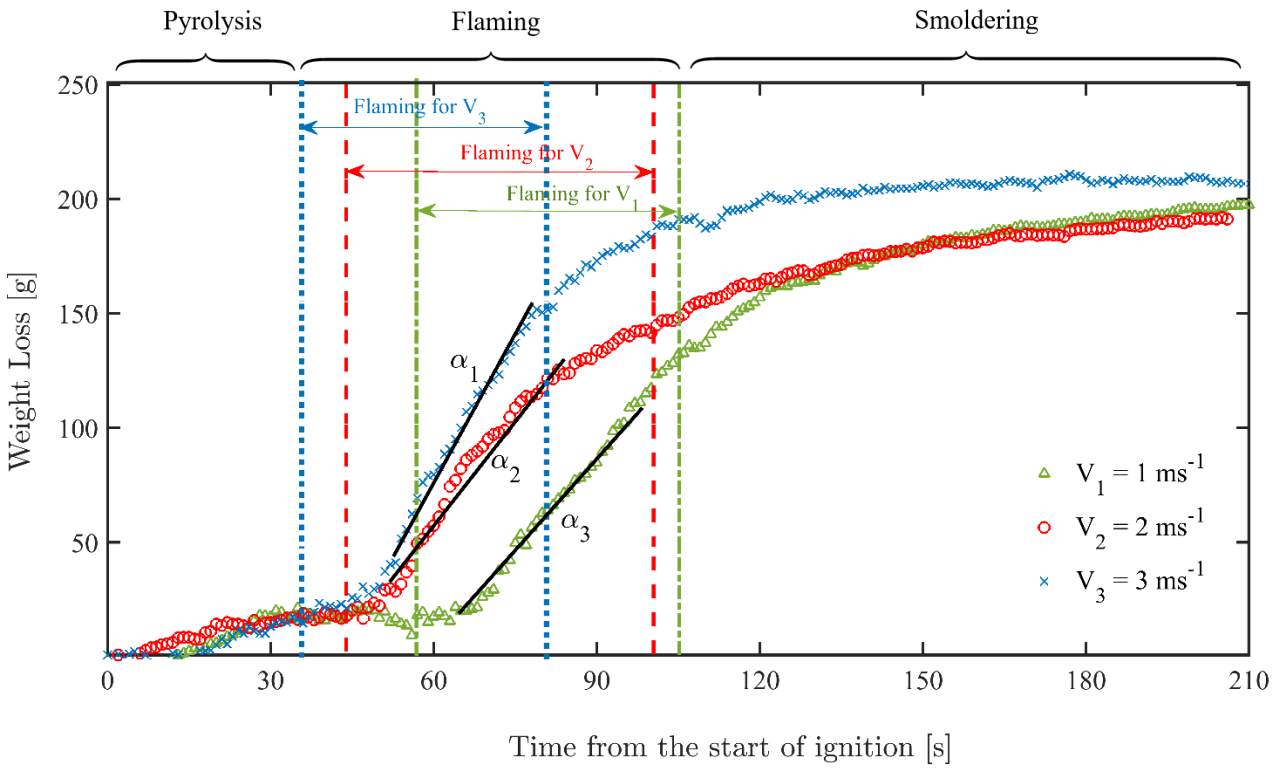

Figure 5. Variation of weight loss over the load cell in three wind velocities.

The weight loss rate (α) was evaluated for the three cases to be 2.8, 2.9, and 4.2 g/s for three velocities of 1,2, and 3m/s respectively. Also, the onset of flaming and smoldering was captured using the two side-view and top-view cameras. These results were presented in Table 2. The duration of pyrolysis and flaming over

the load cell were reduced by increasing the wind velocity, which led to an increase in smoldering time at higher velocity.

Table 2. Weight loss specifications over the course of experiment

Test number	Wind velocity (m/s)	Weight loss (g)	Weight loss rate (g/s)	Duration of pyrolysis (s)	Duration of flaming (s)	Duration of smoldering (s)
Test 1	1	197	2.8	55.8	104.4	105.6
Test 2	2	191.2	2.9	43.2	99.6	110.4
Test 3	3	210.8	4.2	34.8	79.8	130.2

3.3 Temperature variations over the load cell

The temperature variation over the load cell was carried out using the thermocouples discussed in Section 2, and the results are shown in Fig 6. As shown in Fig. 1, the flow is from right to left, hence TC1 to TC3 are positioned upstream with respect to TC4, and TC5. Therefore, it is expected to see TC1 to TC3 facing the flame earlier than TC4, and TC5. Considering the highest temperature to be the flame temperature passing the thermocouples, the peak-to-peak variation reveals an estimate of the flame spread rate.

In Fig. 6(a), TC1, TC2, and TC3 reached the peak at 72,93, and 86 seconds, which represent slight delay relative to the onset of flaming for wind velocity of 1m/s reported in Table 2. This time difference could be due to the time it takes for the flame to reach the depth of the fuel bed. The flame at the surface of the bed was captured by the cameras earlier than it reaches the depth where the thermocouples are located. Estimating the peak-to-peak time interval for TC3 to TC4 (at the edge of the load cell) in Fig. 6(a) leads to approximately 40 sec. Hence, an approximate spread rate can be evaluated to be 1.35 cm/s (at a distance of 55 cm between the TC1-TC3 and TC4-TC5), which is consistent with the spread rate reported Fig 4. However, this rate is slightly increased to 1.8 cm/s for the peak-to-peak evaluation of TC2 to TC5 which are located in the middle of the load cell, hence the fuel bed.

Fig. 6(b) represents the temperature variations for the wind velocity of 2m/s. The peak-to-peak evaluation of spread rate was estimated to be 1.4 cm/s for TC2 to TC5, which rises to 7.8 cm/s for TC3 to TC4. This is the result of a faster spread rate on the right part of the bed relative to the center. These two estimates are slightly different from the spread rate evaluated using image processing (reported in Fig. 4). The coupled flaming-smoldering could be a possible consequent of more flattened peaks of temperatures which could result in overestimation of the spread rate. Another reason could be due to the skewness of flame profile to one side of the bed as a result of the distortions in velocity profile at boundary layer, which has changed the symmetrical wind profile due to vortical flow structures.

At the higher wind velocity of 3m/s in Fig. 6(c), the thermocouple TC4 reaches to the peak of temperature 40 sec earlier than TC3. This phenomenon could be the result of unburnt fuel which are delayed in the flaming process due to the higher convection rate at 3m/s. This behavior increased the chance of discontinuous flaming as opposed to steady flame at the lower velocities. Similar to the peak temperature of the thermocouples showed in Fig 6(b), the flattened peaks were seen to be the dominant feature of most thermocouples in Fig 6(c).

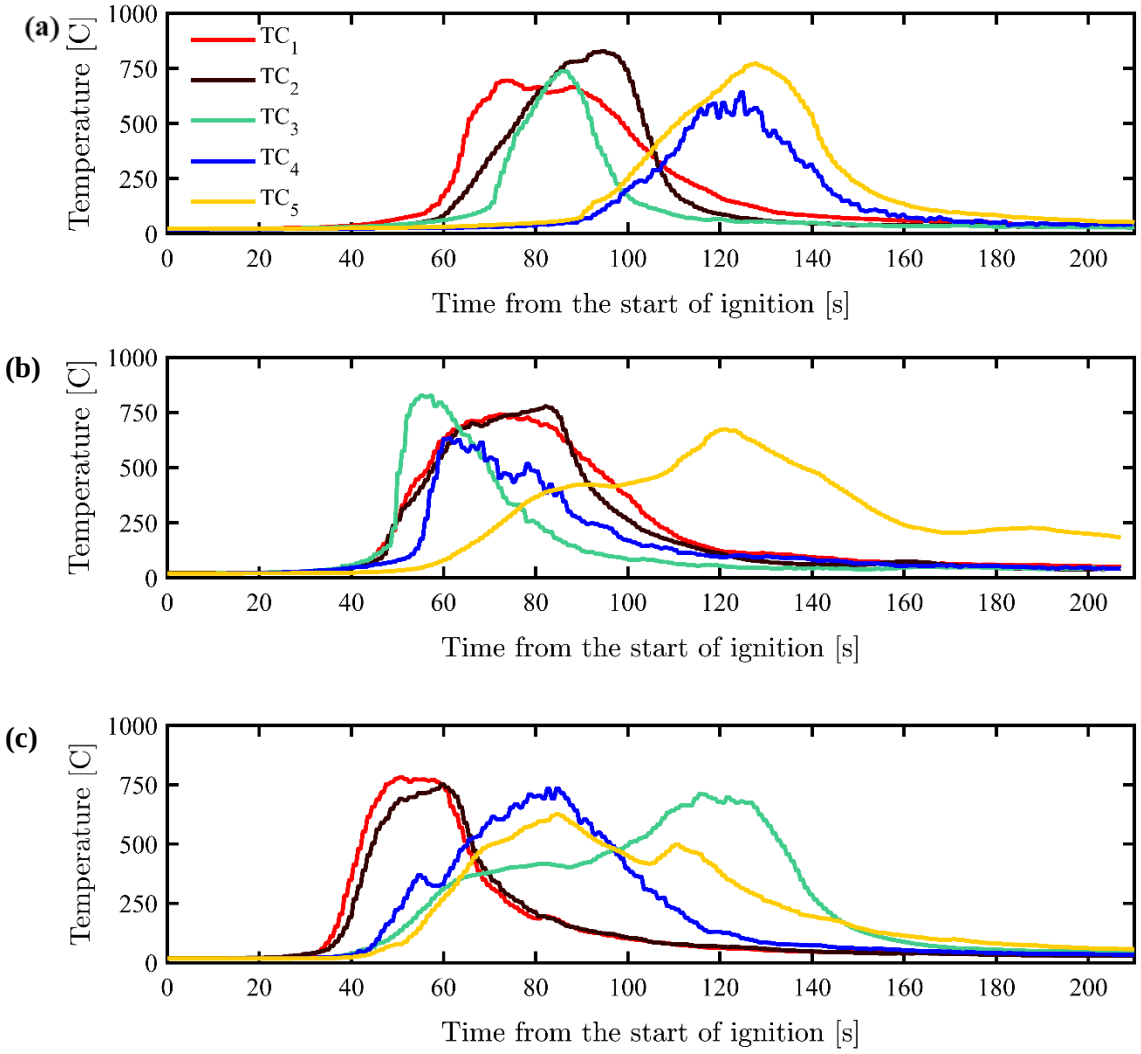

Figure 6. Variation of temperature over the load cell for TC1 to TC5. **(a)** Wind velocity at 1 m/s, **(b)** wind velocity at 2 m/s, and **(c)** wind velocity at 3 m/s.

3.4 Heat flux variations

The heat flux variations for three wind velocities were shown in Fig. 7. Considering the maximum heat flux is when flame passes over the sensor, an estimate of flame spread rate can be achieved using this approximation. Hence the spread rate found from the peak of HF1 and HF2 in Fig 7(a) is 2.75 cm/s which higher than what was evaluated from image processing in Fig. 4. The same approximation for Fig 6(b) leads to a spread rate of 3.6 cm/s for HF1 and HF2. Also, this value is estimated to be 4.2 cm/s for Fig. 7(c), which is double as much as what was calculated using the image processing for the higher wind velocity case. The maximum heat flux for all three cases reaches to 50-60 KW/m^2, which corresponds to values found experimentally by Frankman et al [20-21].

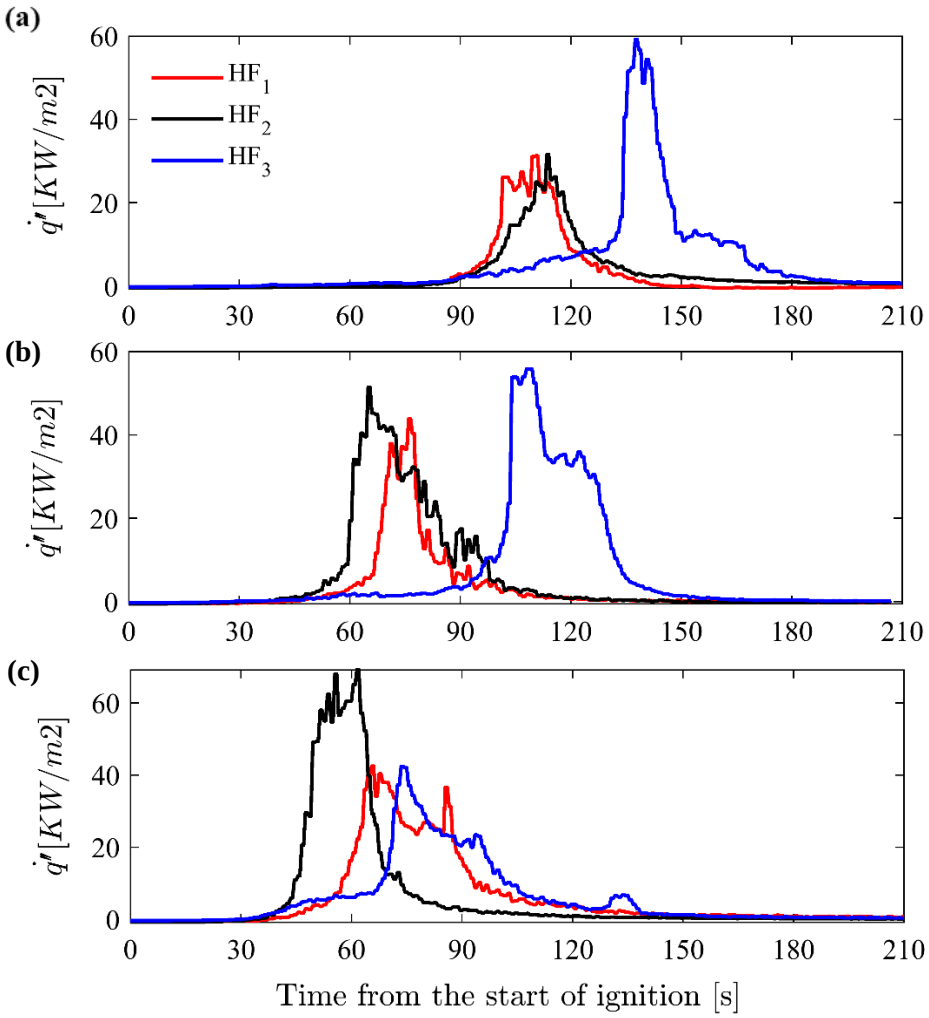

Figure 7. Variation of heat flux at the end of the fuel bed (2.75 m from the ignition pint). **(a)** Wind velocity at 1 m/s, **(b)** wind velocity at 2 m/s, and **(c)** wind velocity at 3 m/s.

4. Conclusion

Wind tunnel testing of a heterogenous fuel bed comprised pine needles was performed at three wind velocities of 1,2, and 3 m/s. Flame behavior and spread rate were consistently coherent with the convective effects of the wind velocities respect to the increased rate of convection, however some differences were observed from estimates of spread rate through image processing versus thermocouples.

Processed flames at the surface of the fuel bed led into finding a linear trend for the spread rate that constantly increased with wind velocity. Detailed comparison of the current study with different beds corresponding to different packing ratio revealed the effect of porosity of the bed on the flame spread as it brings up point of a question for the current study. Also, the flame spread showed a non-uniform behavior at higher velocity cases, which resulted in a faster local spread rates at parts of the bed as opposed to lower velocity cases where the flame spread rate was more uniform throughout the entire bed. This effect could be result of continuous distortion of the boundary layer by the porous bed at higher velocities versus lower velocities, which needs to be further investigated to distinguish between local variation of velocity gradient and turbulent buoyancy-driven flame structures.

Mass loss as well as mass loss rate were investigated at an established flame distance of 2/3 of the overall length of the bed from the point of ignition. The mass consumption occurred earlier in the higher velocities but the total mass was remained approximately unchanged for the three wind velocities of 1,2, and 3m/s.

The spread rate estimated from the maximum of temperature distributions were slightly delayed from the rates calculated based on image processing of the flame at the surface of the fuel bed. A probable speculation arises from the location of thermocouples inside the bed being untouched by the surface of the fuel. Hence, most of the flaming versus smoldering timing were different from what was observed through the image processing. The maximum heat flux in three cases of velocities remained unchanged, however, the estimate of spread rate from the maximum heat flux showed a higher rate as opposed to the processed videos. A time resolved measurement at different heights of the fuel bed is required for a better understanding of the flame spread rate. This study is a significant stage in understating the coupled flame behavior for a heterogeneous bed in the vicinity of wind-driven forced convection.

5. References

[1] Simeoni, A., P. Salinesi, and F. Morandini, Physical modelling of forest fire spreading through heterogeneous fuel beds. International Journal of Wildland Fire, 2011. **20**(5).
[2] Simeoni, A., et al., Flammability studies for wildland and wildland–urban interface fires applied to pine needles and solid polymers. Fire Safety Journal, 2012. **54**: p. 203-217.
[3] Cheney, N.P., J.S. Gould, and W.R. Catchpole, The Influence of Fuel, Weather and Fire Shape Variables on Fire-Spread in Grasslands. International Journal of Wildland Fire, 1993. **3**(1): p. 31-44.
[4] Bartoli, P., et al., Determination of the main parameters influencing forest fuel combustion dynamics. Fire Safety Journal, 2011. **46**(1-2): p. 27-33.
[5] Mendes-Lopes, J.M.C., J.M.P. Ventura, and J.M.P. Amaral, Flame characteristics, temperature-time curves, and rate of spread in fires propagating in a bed of Pinus pinaster needles. International Journal of Wildland Fire, 2003. **12**(1): p. 67-84.
[6] Viegas, D.X., Slope and wind effects on fire propagation. International Journal of Wildland Fire, 2004. **13**(2).
[7] Dupuy, J.L., et al., The effects of slope and fuel bed width on laboratory fire behaviour. International Journal of Wildland Fire, 2011. **20**(2): p. 272-288.
[8] Di Cristina, G., Kozhumal, S., Simeoni, A., Skowronski, N., Rangwala, A. and Im, S.K., 2020. Forced convection fire spread along wooden dowel array. Fire Safety Journal, p.103090.
[9] Di Cristina, G., Skowronski, N. S., Simeoni, A., Rangwala, A. S., & Im, S. K. (2020). Flame spread behavior characterization of discrete fuel array under a forced flow. Proceedings of the Combustion Institute.
[10] Di Cristina, G. (2021). Forced convective flame flow interactions in discrete fuel arrays.
[11] Carey, Jennifer H. 1992. Pinus taeda. In: Fire Effects Information System, [Online]. U.S. Department of Agriculture, Forest Service, Rocky Mountain Research Station, Fire Sciences Laboratory (Producer). Available: https://www.fs.fed.us/database/feis/plants/tree/pintae/all.html [2021, April 4]
[12] Pereira, J. M. C., Sequeira, N. M. S., & Carreiras, J. M. B. (1995). Structural-properties and dimensional relations of some Mediterranean shrub fuels. International Journal of Wildland Fire, 5(1), 35-42.
[13] Fehrmann, S., Jahn, W., & de Dios Rivera, J. (2017). Permeability comparison of natural and artificial pinus radiata forest litters. Fire technology, 53(3), 1291-1308.

[14] Hidalgo, J. P., Maluk, C., Cowlard, A., Abecassis-Empis, C., Krajcovic, M., & Torero, J. L. (2017). A Thin Skin Calorimeter (TSC) for quantifying irradiation during large-scale fire testing. International Journal of Thermal Sciences, 112, 383-394.

[15] Otsu, N., 1979. A threshold selection method from gray-level histograms. IEEE transactions on systems, man, and cybernetics, 9(1), pp.62-66.

[16] Heskestad, G., 1983. Luminous heights of turbulent diffusion flames. Fire safety journal, 5(2), pp.103-108.

[17] Matthews, S., 2010. Effect of drying temperature on fuel moisture content measurements. International Journal of Wildland Fire, 19(6), pp.800-802.

[18] Gould, J.S., Sullivan, A.L., Hurley, R. and Koul, V., 2017. Comparison of three methods to quantify the fire spread rate in laboratory experiments. International journal of wildland fire, 26(10), pp.877-883.

[19] Catchpole, W. R., Catchpole, E. A., Butler, B. W., Rothermel, R. C., Morris, G. A., & Latham, D. J. (1998). Rate of spread of free-burning fires in woody fuels in a wind tunnel. Combustion Science and Technology, 131(1-6), 1-37.

[20] Frankman, D., Webb, B. W., & Butler, B. W. (2010). Time-resolved radiation and convection heat transfer in combusting discontinuous fuel beds. Combustion Science and Technology, 182(10), 1391-1412.

[21] Frankman, D., Webb, B. W., Butler, B. W., Jimenez, D., Forthofer, J. M., Sopko, P., ... & Ottmar, R. D. (2013). Measurements of convective and radiative heating in wildland fires. International Journal of Wildland Fire, 22(2), 157-167.